

Postbuckling Behavior of Longitudinally Compressed Orthotropic Plates with Transverse Shearing Flexibility

Manuel Stein* and Nancy Jane C. Bains†

NASA Langley Research Center, Hampton, Virginia

This paper presents buckling and postbuckling results for plates loaded in compression. The buckling results have been plotted to show the effects of thickness on the stress coefficient for aluminum plates. Results are given for various length-to-width ratios. Postbuckling results for thin plates with transverse shearing flexibility are compared to results from classical theory. The problems considered are the postbuckling response of plates made of aluminum and of a ± 45 deg graphite-epoxy laminate. Thus, the materials are isotropic and orthotropic, respectively. The plates are considered to be long with side edges simply supported, with various in-plane edge conditions, and the plates are subject to a longitudinal compressive displacement. Characteristic curves presenting the average longitudinal direct-stress resultant as a function of the applied displacement are given. These curves indicate that a change in in-plane edge conditions influences plate postbuckling stiffness and that transverse shearing is only important when the plate is thick or the transverse shear stiffness is low.

Nomenclature

| | |
|---|--|
| $A_{11}, A_{12}, A_{22}, A_{33},$ A_{44}, A_{55}, A_{66} | = orthotropic plate extensional stiffnesses |
| a, b, h | = dimensions of rectangular plate parallel to x , y , and z axes, respectively |
| $C_{11}, C_{12}, C_{22}, C_{33},$ C_{44}, C_{55}, C_{66} | = stiffnesses in Hooke's law for each lamina |
| $D_{11}, D_{12}, D_{22}, D_{66}$ | = orthotropic plate bending stiffnesses |
| E | = Young's modulus for material |
| M_y | = bending moment in plate per unit length |
| $M_{y1}, N_{y2}, N_{xy2}, N_{xz1}$ | = functions of y appearing in |

$$M_y = M_{y1} \sin \frac{\pi x}{\lambda}$$

$$N_y = N_{y2} \cos \frac{2\pi x}{\lambda}$$

$$N_{xy} = N_{xy2} \sin \frac{2\pi x}{\lambda}$$

$$N_{xz} = N_{xz1} \cos \frac{\pi x}{\lambda}$$

| | |
|-----------------------|---|
| N_x, N_y, N_{xy} | = in-plane stress resultants in plate |
| N_{xz}, N_{yz}, N_z | = transverse stress resultants in plate |

| | |
|----------------------|--|
| N_{xav} | = average compressive load per unit length |
| N_{xcr} | = value of N_{xav} at buckling |
| U | = applied end shortening |
| U_{cr} | = value of U at buckling |
| V_y, β_y | = functions of x and y defined in the "Results and Discussion" section |
| V_{y1}, β_{y1} | = functions of y defined by |

$$V_y = V_{y1} \cos \frac{\pi x}{\lambda}$$

$$\beta_y = \beta_{y1} \cos \frac{\pi x}{\lambda}$$

| | |
|---|---|
| u, v, w | = displacements in x , y , and z directions, respectively |
| u_2^0, v_2^0, w_1^0 | = functions of y appearing in Eqs. (3) |
| x, y, z | = plate coordinates |
| $\epsilon_x, \epsilon_y, \epsilon_z, \gamma_{yz}, \gamma_{xz}, \gamma_{xy}$ | = strains in plate |
| λ | = buckle half-wavelength |
| μ | = Poisson's ratio for material |
| $\sigma_x, \sigma_y, \sigma_z, \tau_{yz}, \tau_{xz}, \tau_{xy}$ | = stresses in each lamina |

Introduction

FOR linear problems, classical plate theory predicts in-plane stresses and deformation that are comparable to those given by three-dimensional elasticity for thin plates of a homogeneous material. Conventional transverse shearing theory makes similar predictions for sandwich construction and for thicker plates of homogeneous material. Transverse stresses are generally smaller compared to the largest in-plane stress; however, they can be important when the plate is relatively weak in the transverse direction and when the plate response is sensitive to the transverse stiffness, as in buckling and higher modes of vibrations.

Classical plate theory and conventional transverse shearing plate theory are two-dimensional, and they predict in-plane stresses directly, but they are not accurate enough to predict transverse stresses directly. An accurate nonlinear two-dimensional theory for laminated and thick plates with three-dimensional flexibility was derived in Ref. 1. The essential difference

Presented as Paper 86-0976 at the AIAA/ASME/ASCE/AHS 27th Structures, Structural Dynamics, and Materials Conference, San Antonio, TX, May 19-21, 1986; received July 15, 1986; revision received Jan. 22, 1989. Copyright © 1989 American Institute of Aeronautics and Astronautics, Inc. No copyright is asserted in the United States under Title 17, U.S. Code. The U.S. Government has a royalty-free license to exercise all rights under the copyright claimed herein for Governmental purposes. All other rights are reserved by the copyright owner.

*Senior Aerospace Engineer, Structural Mechanics Branch, Structural Mechanics Division, Associate Fellow AIAA.

†Mathematician, Structural Mechanics Branch, Structural Mechanics Division.

between this theory and classical theory or conventional transverse shearing theory is the use of trigonometric terms in addition to the usual constant and linear terms that represent the through-the-thickness variation of the displacements. This new theory was applied to cylindrical bending plate problems in Ref. 2 to show that the theory can predict directly the transverse stresses as well as the in-plane stresses. The purpose of the present paper is to present the results of the buckling of thick, rectangular, simply supported aluminum plates in compression and to determine if the plate postbuckling response for thin plates is sensitive to transverse shearing flexibility and to present postbuckling results for long, thin, simply supported plates in compression. Deflections, transverse shearing stresses, and characteristic curves presenting the average compressive stress resultant as a function of the applied displacement are given for a wide variety of in-plane edge conditions.

Analysis

The derivation of the equations to be solved using classical (Kirchoff) theory was presented in Ref. 3. The derivation of equations using conventional transverse shearing theory and three-dimensional flexibility theory follows similarly and, accordingly, is not presented here in detail. Using all three theories allows one to decide which approximation is needed to provide reasonably accurate results for the range of variables treated.

To help one understand the differences between the various theories, it is convenient to start with the most complicated theory, then neglect or change terms to get to the least complicated theory. For the three-dimensional flexibility theory, the displacements are (from Eq. 24 of Ref. 1)

$$\begin{aligned} u(x, y, z) &= u^0(x, y) + u^a(x, y) \frac{z}{h} + u^s(x, y) \sin \frac{\pi z}{h} \\ v(x, y, z) &= v^0(x, y) + v^a(x, y) \frac{z}{h} + v^s(x, y) \sin \frac{\pi z}{h} \\ w(x, y, z) &= w^0(x, y) + w^c(x, y) \cos \frac{\pi z}{h} \end{aligned} \quad (1)$$

and the nonlinear strains corresponding to these displacements are taken to be (from Eq. 25 of Ref. 1)

$$\begin{aligned} \epsilon_x &= u_{,x}^0 + \frac{1}{2} w_{,x}^{02} + u_{,x}^a \frac{z}{h} + u_{,x}^s \sin \frac{\pi z}{h} \\ \epsilon_y &= v_{,y}^0 + \frac{1}{2} w_{,y}^{02} + v_{,y}^a \frac{z}{h} + v_{,y}^s \sin \frac{\pi z}{h} \\ \epsilon_z &= -\frac{\pi}{h} w^c \sin \frac{\pi z}{h} \\ \gamma_{xy} &= u_{,y}^0 + v_{,x}^0 + w_{,xy}^0 + (u_{,y}^a + v_{,x}^a) \frac{z}{h} + (u_{,y}^s + v_{,x}^s) \sin \frac{\pi z}{h} \\ \gamma_{xz} &= w_{,x}^0 + \frac{u^a}{h} + \left(w_{,x}^c + \frac{\pi}{h} u^s \right) \cos \frac{\pi z}{h} \\ \gamma_{yz} &= \frac{v^a}{h} + w_{,y}^0 + \left(\frac{\pi}{h} v^s + w_{,y}^c \right) \cos \frac{\pi z}{h} \end{aligned} \quad (2)$$

For conventional transverse shearing theory, the trigonometric terms are absent. In classical plate theory, the trigonometric terms are also absent and u^a/h and v^a/h are replaced by $-w_{,x}^0$ and $-w_{,y}^0$, respectively, to satisfy the Kirchhoff assumption that lines normal to the undeformed neutral surface remain normal to the neutral surface after deformation.

Guided by Refs. 3 and 4, the form of the unknown displacements is

$$\begin{aligned} u^0 &= -U \left(\frac{x}{a} - \frac{1}{2} \right) + u_2^0(y) \sin \frac{2\pi x}{\lambda} \\ v^0 &= v_0^0(y) + v_2^0(y) \cos \frac{2\pi x}{\lambda} \\ u^a &= u_1^a(y) \cos \frac{\pi x}{\lambda}, \quad v^a = v_1^a(y) \sin \frac{\pi x}{\lambda} \\ u^s &= u_1^s(y) \cos \frac{\pi x}{\lambda}, \quad v^s = v_1^s(y) \sin \frac{\pi x}{\lambda} \\ w^0 &= w_1^0(y) \sin \frac{\pi x}{\lambda} \\ w^c &= w_1^c(y) \sin \frac{\pi x}{\lambda} \end{aligned} \quad (3)$$

The transverse displacement w and the bending parts of u and v , which are all exact at buckling, are sinusoidally periodic with half-wavelength γ . The extensional parts of u and v , i.e., u^0 and v^0 , are sinusoidally periodic with half-wavelength $\lambda/2$, and u^0 has an extra linear-in- x term associated with the constant U that is the applied displacement and, therefore, specified.

The virtual work of the internal forces for a three-dimensional body is

$$\begin{aligned} \delta \Pi &= \int_0^a \int_0^b \int_{-h/2}^{h/2} (\sigma_x \delta \epsilon_x + \sigma_y \delta \epsilon_y + \sigma_z \delta \epsilon_z + \tau_{xy} \delta \gamma_{xy} \\ &\quad + \tau_{xz} \delta \gamma_{xz} + \tau_{yz} \delta \gamma_{yz}) dx dy dz \end{aligned} \quad (4)$$

For the cases treated here, Hooke's law for the relation of stresses to strains for each lamina is taken to be

$$\begin{Bmatrix} \sigma_x \\ \sigma_y \\ \sigma_z \\ \tau_{yz} \\ \tau_{xz} \\ \tau_{xy} \end{Bmatrix} = \begin{Bmatrix} C_{11} & C_{12} & 0 & 0 & 0 & 0 \\ C_{12} & C_{22} & 0 & 0 & 0 & 0 \\ 0 & 0 & 0 & C_{33} & 0 & 0 \\ 0 & 0 & 0 & C_{44} & 0 & 0 \\ 0 & 0 & 0 & 0 & C_{55} & 0 \\ 0 & 0 & 0 & 0 & 0 & C_{66} \end{Bmatrix} \begin{Bmatrix} \epsilon_x \\ \epsilon_y \\ \epsilon_z \\ \gamma_{yz} \\ \gamma_{xz} \\ \gamma_{xy} \end{Bmatrix} \quad (5)$$

Stress and moment resultants may be defined. Examples are

$$\begin{aligned} N_y &= \int_{-h/2}^{h/2} \sigma_y dz = N_y^0 + N_y^2 \cos \frac{2\pi x}{\lambda} \\ M_y &= \int_{-h/2}^{h/2} \sigma_y z dz = M_y^1 \sin \frac{\pi x}{\lambda} \end{aligned}$$

Differential equations and variationally consistent boundary conditions were derived from the virtual work in much the same way as for classical theory in Ref. 3 for the conventional transverse shearing theory and for the three-dimensional flexibility theory. Computer programs were written for these two additional cases. The detailed boundary conditions at $y = 0, b$ used were

Classical

$$u_2^0 = 0, \quad \begin{Bmatrix} v_0^0 \\ N_y^0 \end{Bmatrix} = 0, \quad \begin{Bmatrix} v_2^0 \\ N_y^2 \end{Bmatrix} = 0, \quad w^0 = 0, \quad M_y^1 = 0$$

Conventional transverse shearing

$$u_2^0 = 0, \quad u_1^a = 0, \quad \left\{ \begin{matrix} v_0^0 \\ N_y^0 \end{matrix} \right\} = 0, \quad \left\{ \begin{matrix} v_2^0 \\ N_y^2 \end{matrix} \right\} = 0, \quad w^0 = 0, \quad M_y^1 = 0 \quad (6)$$

Three-dimensional flexibility

$$\begin{aligned} u_2^0 &= 0, \quad u_1^a = 0, \quad u_1^i = 0, \quad \left\{ \begin{matrix} v_0^0 \\ N_y^0 \end{matrix} \right\} = 0, \quad \left\{ \begin{matrix} v_2^0 \\ N_y^2 \end{matrix} \right\} = 0 \\ w^0 &= 0, \quad w^c = 0 \\ M_y^1 &= 0, \quad L_y = 0 \end{aligned}$$

where

$$L_y = \int_{-h/2}^{h/2} \sigma_y \sin \frac{\pi z}{h} dz$$

The half-wavelength λ of interest for the infinitely long plates considered here is the one that corresponds to minimum energy, and the solution of interest is on the equilibrium path that gives nonzero deflections.

Results and Discussion

The results obtained in this study for aluminum plates are based on the thickness $h = 1$ in. and with the mechanical properties of $E = 10.7 \times 10^6$ psi and $\mu = 0.33$. Buckling results for an aluminum plate are presented in Fig. 1, taken from Ref. 1. The results presented in Fig. 1 show the variation of the buckling stress coefficient with thickness ratio as given by the three theories (classical, conventional transverse shearing, and three-dimensional flexibility) for a range of length-width aspect ratios. These results show that for aluminum plates with a thickness greater than 10% of the plate width, the effects of transverse shearing should be included in determin-

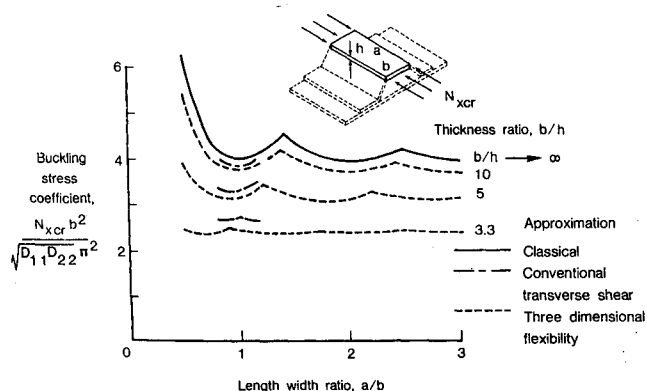


Fig. 1 Effect of thickness on the buckling stress coefficient for aluminum plates.

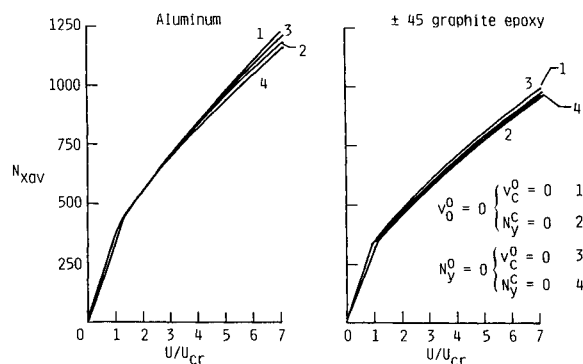


Fig. 2 Characteristic curves for postbuckling of long rectangular plates in compression.

ing the compressive buckling stress. This lower buckling stress would be important in determining the buckling load of the crown of a hat stiffener in a stiffened panel in bending or compression and the start of postbuckling. However, a closer look at these results shows that, at best, for thickness ratios of interest (for thicker plates), the buckling stresses are near or above the elastic limit and elastic postbuckling studies could only serve as a guide. Accordingly, the postbuckling results presented here in order to be of practical use will be directed toward plates with thickness ratios b/h greater than 10. Therefore, from the results of Fig. 1, it would seem that only classical theory would be needed.

Characteristic curves are presented in Fig. 2 for the postbuckling in compression of rectangular plates made of aluminum and ± 45 deg graphite-epoxy, respectively. The average longitudinal in-plane stress corresponding to the applied longitudinal in-plane displacement is plotted in terms of dimensionless parameters for an infinitely long plate. Curves were obtained from all three theories. Shown is only one curve that represents classical theory, conventional transverse shearing theory, and the three-dimensional flexibility theory since they were essentially equivalent. The ± 45 deg graphite-epoxy laminate has the dimensions $h = 0.1$ in. and $b = 10$ in. and the following properties (the units of D 's are in./lb and the units of A 's lb/in.):

$$\begin{aligned} A_{11} - A_{22} &= 0.62034 \times 10^6 & D_{11} &= D_{22} = 0.5186 \times 10^3 \\ A_{33} &= 0.59 \times 10^5 \\ A_{12} &= 0.44606 \times 10^6 & D_{12} &= 0.37291 \times 10^3 \\ A_{44} &= A_{55} = 0.5 \times 10^5 \\ A_{66} &= 0.48352 \times 10^6 & D_{66} &= 0.40423 \times 10^3 \end{aligned}$$

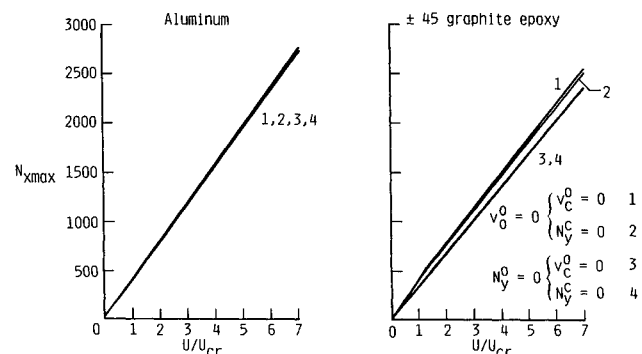


Fig. 3 Maximum N_x stress for postbuckling of long rectangular plates in compression.

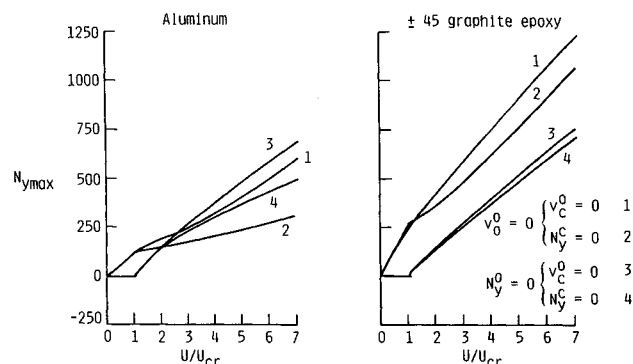


Fig. 4 Maximum N_y stress for postbuckling of long rectangular plates in compression.

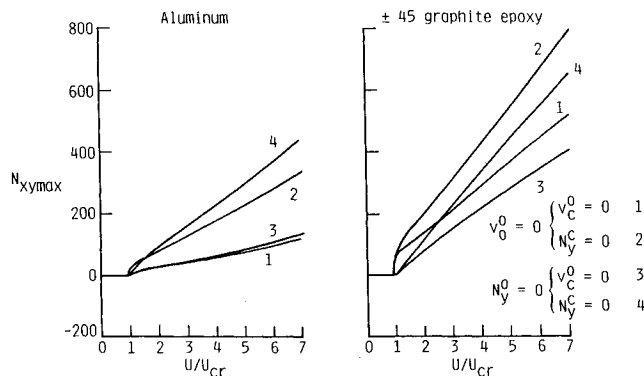


Fig. 5 Maximum N_{xy} stress for postbuckling of long rectangular plates in compression.

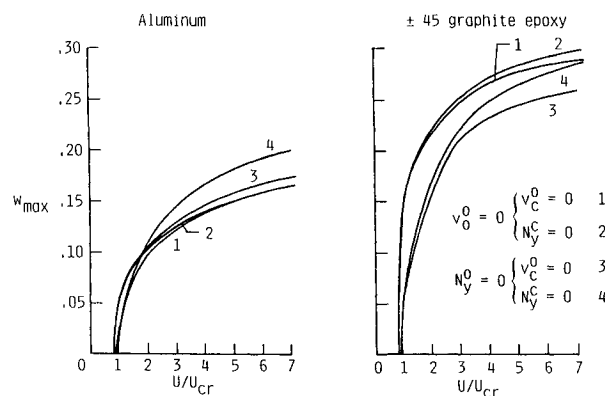


Fig. 6 Maximum deflection for postbuckling of long rectangular plates in compression.

Again, even for lower values of the transverse shearing stiffness A_{44} and A_{55} and the direct transverse stiffness A_{33} , the results in Fig. 1 from classical theory gave the same results for N_{xav} for this thinner plate as higher-order theories. Similar results were also obtained for the maximum compressive stress $N_{x,max}$ in Fig. 3, the maximum stress $N_{y,max}$ in Fig. 4, the maximum shear stress $N_{xy,max}$ in Fig. 5, and the maximum deflection w_{max} in Fig. 6. Boundary conditions make a difference in most of the curves. However, other results of this analysis show that conventional transverse shearing theory was needed to obtain transverse shear loads for the ± 45 deg composite plate such as the values of $N_{xz,max}$ presented in Fig. 7 at the applied displacement u equal to 7 times the critical value of u . The $N_{xz,max}$ for the aluminum plate were much smaller. Also, for the boundary conditions that the edges

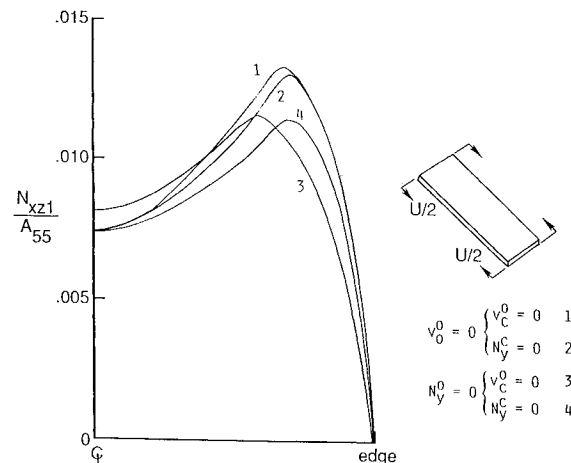


Fig. 7 Transverse shearing stress distribution at $U/V_{cr} = 7$ of long rectangular ± 45 graphite epoxy plates in compression.

remain straight, it was found that conventional shearing theory was needed to obtain more accurate in-plane displacements and force resultants.

Concluding Remarks

Previous results have shown that for thin plates and for linear and buckling problems, classical (Kirchoff) theory gave adequate results. When plates are thicker, more accurate theories like the conventional transverse shearing theory or three-dimensional flexibility theory are required. Beyond buckling, when the deformations become large and thicker plates pass into the plastic range, some thinner plates develop considerable transverse shearing strains (which were assumed to be zero by the Kirchoff assumption), as shown by the present results for the ± 45 deg graphite-epoxy laminated plate. The present results also show that classical theory is accurate for maximum force resultants and deflections for a variety of in-plane boundary conditions for both aluminum and ± 45 deg graphite-epoxy, laminated, simply supported plate.

References

- Stein, M., "Nonlinear Theory for Laminated and Thick Plates and Shells Including the Effects of Transverse Shearing," *AIAA Journal*, Vol. 24, Sept. 1986 pp. 1537-1544.
- Stein, M. and Jegley, D. C., "Effects of Transverse Shearing on Cylindrical Bending, Vibration and Buckling of Laminated Plates," *AIAA Paper 85-0744 CP*, April 1985.
- Stein, M., "Postbuckling of Orthotropic Composite Plates Loaded in Compression," *AIAA Journal*, Vol. 21, Dec. 1983, pp. 1729-1735.
- Stein, M., "Loads and Deformations of Buckled Rectangular Plates," *NASA TR R-40*, 1959.